Supporting Information

Photoreforming of non-recyclable plastic waste over a carbon nitride/nickel phosphide catalyst

Taylor Uekert, Hatice Kasap, Erwin Reisner*

Christian Doppler Laboratory for Sustainable SynGas Chemistry, Department of Chemistry, University of Cambridge, Lensfield Road, Cambridge CB2 1EW, UK. *e-mail: reisner@ch.cam.ac.uk

List of abbreviations

CN_x – cyanamide-functionalized carbon nitride

$^{H_2N}CN_x$ – unfunctionalized carbon nitride

EG – ethylene glycol

LA – lactic acid

Ni_2P – nickel phosphide

PE – polyethylene

PET – polyethylene terephthalate

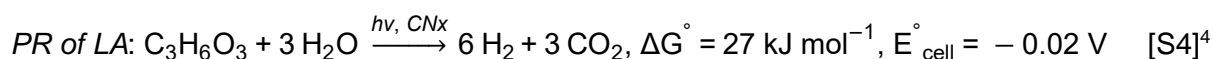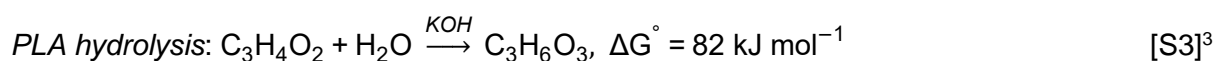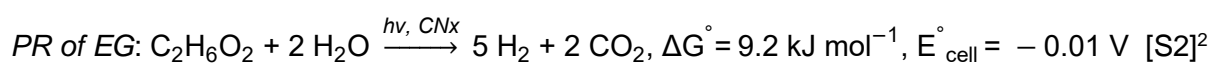PLA – polylactic acid
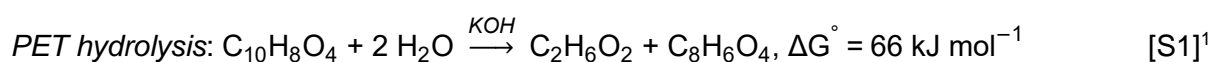
PP – polypropylene

PR – photoreforming

PS – polystyrene

PUR – polyurethane

Rubber – polystyrene-block-polybutadiene

Thermodynamic calculations

Gibbs free energies were obtained or calculated from data in the cited references:

PET hydrolysis: $C_{10}H_8O_4$ + 2 H_2O $\xrightarrow{KOH}$ $C_2H_6O_2$ + $C_8H_6O_4$, $\Delta G^° = 66$ kJ mol^{-1} [S1][1]

PR of EG: $C_2H_6O_2$ + 2 H_2O $\xrightarrow{hv,\ CNx}$ 5 H_2 + 2 CO_2, $\Delta G^° = 9.2$ kJ mol^{-1}, $E^°_{cell} = -0.01$ V [S2][2]

PLA hydrolysis: $C_3H_4O_2$ + H_2O $\xrightarrow{KOH}$ $C_3H_6O_3$, $\Delta G^° = 82$ kJ mol^{-1} [S3][3]

PR of LA: $C_3H_6O_3$ + 3 H_2O $\xrightarrow{hv,\ CNx}$ 6 H_2 + 3 CO_2, $\Delta G^° = 27$ kJ mol^{-1}, $E^°_{cell} = -0.02$ V   [S4][4]

Supplementary Tables

Table S1. Inductively coupled plasma optical emission spectrometry (ICP-OES) quantification of Ni and P content of several catalysts. Samples (typically ~ 3mg) were dissolved in 2 mL of 2:1 $H_2O_2:H_2SO_4$ overnight, diluted with H_2O and then submitted for measurement.

Catalyst	Ideal Ni content (mg_{Ni} g_{CNx}^{-1})	Measured Ni content (mg_{Ni} g_{CNx}^{-1})	Ideal P content (mg_P g_{CNx}^{-1})	Measured P content (mg_P g_{CNx}^{-1})
$CN_x|Ni_2P$	15.9	15.3	4.2	52.2
$CN_x|Ni_2P$ post-PR	15.9	15.1	4.2	8.8
solution post-PR[a]	0.00	0.14	n.m.	n.m.
CN_x-P[b]	--	--	5.0	40.3
CN_x-PO_x[c]	--	--	4.9	35.4
$^{H2N}CN_x$-P[b]	--	--	5.0	14.0

n.m. = not measured

[a] The photocatalyst was removed *via* centrifugation, and only the supernatant was submitted for ICP analysis.

[b] CN_x-P and $^{H2N}CN_x$-P were synthesized according to the $CN_x|Ni_2P$ procedure, but *without* the addition of the Ni precursor.

[c] CN_x-PO_x was prepared by replacing $NaH_2PO_2 \cdot H_2O$ with Na_3PO_4 in the above synthesis.

Table S2. X-ray photoelectron spectroscopy (XPS) survey quantification of CN_x, Ni_2P, $CN_x|Ni_2P$ (2 wt%), post-catalysis $CN_x|Ni_2P$ (2 wt%), and $CN_x|P$. All powders were dispersed in ethanol and drop-cast on FTO glass slides prior to characterization.

Sample	Atomic concentration (%)					
	O 1s	C 1s	N 1s	K 2s	Ni $2p_{3/2}$	P 2p
CN_x area 1	12.54	34.33	41.38	5.89	--	--
CN_x area 2	23.37	27.85	30.89	5.08	--	--
CN_x area 3	17.75	33.63	34.79	5.24	--	--
Average	17.89	31.94	35.69	5.40	--	--
Ni_2P area 1	47.82	20.21	--	--	4.67	17.90
Ni_2P area 2	41.26	30.02	--	--	4.18	16.74
Ni_2P area 3	46.59	20.55	--	--	5.50	21.50
Average	45.22	23.59	--	--	4.78	18.71
$CN_x|Ni_2P$ area 1	13.09	35.18	39.17	3.80	0.37	1.93
$CN_x|Ni_2P$ area 2	18.76	31.46	34.90	3.94	0.25	1.38
$CN_x|Ni_2P$ area 3	14.73	33.74	38.48	4.01	0.30	1.75
Average	15.53	33.46	37.52	3.92	0.31	1.69
Post-PR $CN_x|Ni_2P$ area 1	29.07	26.06	24.81	1.15	0.19	--
Post-PR $CN_x|Ni_2P$ area 2	27.65	27.36	25.90	1.84	0.18	--
Post-PR $CN_x|Ni_2P$ area 3	23.95	29.01	29.89	1.62	0.28	--
Average	26.89	27.48	26.87	1.54	0.22	--
$CN_x|P$ area 1	7.59	40.66	42.76	3.91	--	1.54
$CN_x|P$ area 2	6.71	41.10	43.48	4.20	--	1.88
Average	7.15	40.88	43.12	4.05	--	1.71

Table S3. Comparison of the synthesized $CN_x|Ni_2P$ catalyst to reported $^{H2N}CN_x|Ni_2P$ catalysts for H_2 evolution with triethanolamine as hole scavenger. All cited samples were irradiated with 300 W Xe lamps with $\lambda > 420$ nm cutoff filters (no temperatures cited). Samples labelled as "this work" were irradiated with a 1000 W Xe lamp (AM 1.5G, 100 mW cm^{-2}, 25 °C) with a $\lambda > 420$ nm cutoff filter.

Catalyst	[Catalyst] (mg mL^{-1})	[Substrate] (mg mL^{-1})	Reactor Volume (mL)	Time (h)	Yield ± σ (μmol$_{H_2}$ g$_{sub}^{-1}$)	Activity ± σ (μmol$_{H_2}$ g$_{cat}^{-1}$ h^{-1})	Ref
$CN_x|Ni_2P$ 2%[a]	1.2	113	7.91	20	33.4 ± 1.7	118 ± 6.0	*
$^{H2N}CN_x|Ni_2P$ 2%	0.83	113	60	20	29.5	200	5
$^{H2N}CN_x|Ni_2P$ 2%	1.2	113	7.91	20	27.4 ± 1.4	96.7 ± 4.9	*
$^{H2N}CN_x|Ni_2P$ 3%	1.0	226	100	4	26.6	1503	6
$^{H2N}CN_xNi_{12}P_5$ 2%	1.0	113	80	20	14.6	82.5	7
$^{H2N}CN_x|Ni_2P$ 3.5%	0.45	103	250	4	8.39	474	8
$^{H2N}CN_x|Ni_2P$ 0.48%	1.0	113	37	2	10.2	575	9
$^{H2N}CN_x|Ni_2P$ 2%	0.5	170	100	3	1.12	127	10

[a] Percentages indicate wt%.
* This work.

Table S4. Optimisation of photoreforming conditions with $CN_x|Ni_2P$. Conditions (unless stated otherwise below): ultra-sonicated $CN_x|Ni_2P$ 2 wt% (3.2 mg), pre-treated PET (50 mg), aqueous KOH (1 M, 2 mL), sealed photoreactor (internal volume 7.91 mL) under anaerobic conditions, simulated solar light (20 h AM 1.5G, 100 mW cm^{-2}, 25 °C). Yields and activities are cumulative values. σ is the standard deviation calculated from 3 samples, unless stated otherwise.

Description	Ni_2P loading (wt %)	Yield ± σ (μmol_{H_2} g_{sub}^{-1})	Activity ± σ (μmol_{H_2} g_{cat}^{-1} h^{-1})
Ni_2P concentration optimisation	0.5	2.11 ± 0.13	1.59 ± 0.10
	2	27.6 ± 3.4	21.6 ± 2.7
	5	29.4 ± 1.5	23.0 ± 1.2

Description	$[CN_x|Ni_2P]$ (mg mL^{-1})	Yield (μmol_{H_2} g_{sub}^{-1})	Activity (μmol_{H_2} g_{cat}^{-1} h^{-1})
CN_x concentration optimisation	0.2[a]	0.980 ± 0.300	6.12 ± 1.87
	0.5[a]	1.45 ± 0.25	3.62 ± 0.62
	1[a]	7.30 ± 0.36	9.12 ± 0.46
	1.6	27.6 ± 3.4	21.6 ± 2.7
	2[a]	22.1 ± 1.1	13.8 ± 0.7

Description	[KOH] (M)	Yield ($mmol_{H_2}$ g_{sub}^{-1})	Activity (μmol_{H_2} g_{cat}^{-1} h^{-1})
KOH concentration optimisation	0	0.0 ± 0.0	0.0 ± 0.0
	0.5	0.800 ± 0.007	0.625 ± 0.005
	1	27.6 ± 3.4	21.6 ± 2.7
	5	83.8 ± 5.3	65.4 ± 2.2
	10	111 ± 8	86.5 ± 6.2

[a] σ calculated from 2 samples.

Table S5. Comparison of photoreforming with pre-treated versus non-treated PET. Conditions: ultra-sonicated $CN_x|Ni_2P$ 2 wt% (3.2 mg), PET (50 mg), aq. KOH (1 M, 2 mL), sealed photoreactor (internal volume 7.91 mL) under anaerobic conditions, simulated solar light (AM 1.5G, 100 mW cm^{-2}, 25 °C). Yields and activities are cumulative values. σ is the standard deviation calculated from 3 samples.

Description	Time (h)	Yield ± σ (μmol_{H_2} g_{sub}^{-1})	Activity ± σ (μmol_{H_2} g_{cat}^{-1} h^{-1})
No pre-treatment	4	5.00 ± 0.34	19.5 ± 1.3
	20	17.1 ± 0.9	12.8 ± 0.6
	22	18.8 ± 1.7	12.8 ± 1.1
With pre-treatment	4	5.06 ± 0.34	19.8 ± 1.3
	20	27.6 ± 3.4	21.6 ± 2.7
	22	30.6 ± 6.1	21.7 ± 4.3

Table S6. Quantification (by ^{1}H-NMR spectroscopy) of polymer solubilization after pre-treatment (before photocatalysis).

Sample	Components	Ideal quantity of component (mg)	Measured quantity of component (mg)	% solubilization
PET	ethylene glycol	2.1	1.3	62
	terephthalate	5.7	2.9	51
PLA	lactate	6.0	4.3	72
PET bottle	ethylene glycol	1.2	0.7	58
	terephthalate	3.1	1.3	42
Polyester fiber	ethylene glycol	1.2	0.3	25
	terephthalate	3.1	0.8	26

Table S7. Comparison of photoreforming with ultra-sonicated versus un-sonicated $CN_x|Ni_2P$. Conditions: $CN_x|Ni_2P$ 2 wt% (3.2 mg), pre-treated PET (50 mg), aq. KOH (1 M, 2 mL), sealed photoreactor (internal volume 7.91 mL) under anaerobic conditions, simulated solar light (AM 1.5G, 100 mW cm^{-2}, 25 °C). Yields and activities are cumulative values. σ is the standard deviation calculated from 3 samples.

Description	Time (h)	Yield $\pm \sigma$ (μmol_{H_2} g_{sub}^{-1})	Activity $\pm \sigma$ (μmol_{H_2} g_{cat}^{-1} h^{-1})
No sonication	4	3.86 ± 0.19	15.1 ± 0.7
	20	6.34 ± 0.44	4.95 ± 0.35
With ultra-sonication	4	5.06 ± 0.34	19.8 ± 1.3
	20	27.6 ± 3.4	21.6 ± 2.7

Table S8. Control experiments for photoreforming of polymers over $CN_x|Ni_2P$. Conditions (unless stated otherwise below): ultra-sonicated $CN_x|Ni_2P$ 2 wt% (3.2 mg), pre-treated polymer (50 mg), aqueous KOH (1 M, 2 mL), sealed photoreactor (internal volume 7.91 mL) under anaerobic conditions, simulated solar light (AM 1.5G, 100 mW cm^{-2}, 25 °C). Yields and activities are cumulative values. σ is the standard deviation calculated from 3 samples.

Description	Time (h)	Yield $\pm \sigma$ (μmol_{H_2})	Activity (μmol_{H_2} g_{cat}^{-1} h^{-1})
No substrate[a,b]	2	0.049 ± 0.021	7.66 ± 3.28
	4	0.053 ± 0.044	4.14 ± 3.44
	20	0.132 ± 0.065	2.06 ± 1.01
	25	0.134 ± 0.011	1.67 ± 0.14
	27	0.145 ± 0.013	1.68 ±0.15
	44	0.171 ± 0.016	1.21 ± 0.11
	46	0.175 ± 0.016	1.19 ± 0.11
	50	0.180 ± 0.017	1.12 ± 0.11
	24	0.071 ± 0.003	0.924 ± 0.046
	48	0.074 ± 0.011	0.482 ± 0.072
	72	0.140 ± 0.010	0.608 ± 0.043
	96	0.208 ± 0.023	0.677 ± 0.075
	120	0.269 ± 0.059	0.700 ± 0.153

Description	Substrate	Time (h)	Yield (μmol_{H_2} g_{sub}^{-1})	Activity (μmol_{H_2} g_{cat}^{-1} h^{-1})
No light	PET	4	0.0 ± 0.0	0.0 ± 0.0
		20	0.0 ± 0.0	0.0 ± 0.0
	PLA	4	0.0 ± 0.0	0.0 ± 0.0
		20	0.0 ± 0.0	0.0 ± 0.0
No catalyst	PET	4	0.0 ± 0.0	0.0 ± 0.0
		20	0.0 ± 0.0	0.0 ± 0.0
	PLA	4	0.0 ± 0.0	0.0 ± 0.0
		20	0.0 ± 0.0	0.0 ± 0.0
No co-catalyst (CN_x only)	PET	4	0.0 ± 0.0	0.0 ± 0.0
		20	0.687 ± 0.034	0.537 ± 0.027
	PLA	4	0.0 ± 0.0	0.0 ± 0.0
		20	1.24 ± 0.22	0.969 ± 0.172
No light-absorber (Ni_2P only)	PET	4	0.0 ± 0.0	0.0 ± 0.0
		20	0.0 ± 0.0	0.0 ± 0.0
	PLA	4	0.0 ± 0.0	0.0 ± 0.0
		20	0.0 ± 0.0	0.0 ± 0.0
Irradiated with λ > 420 nm filter	PET	4	3.96 ± 0.54	15.5 ± 2.1
		20	5.52 ± 0.74	4.31 ± 0.58
	PLA	4	4.76 ± 0.24	18.6 ± 0.9
		20	10.9 ± 0.7	8.54 ± 0.56

[a] Different samples were used for the 2-50 h and 24-120 h timescales.
[b] The high initial activity is likely due to remnant NaH_2PO_2 from Ni_2P co-catalyst synthesis.

Table S9. Screening of noble-metal-free co-catalysts with CN_x for photoreforming of PET. Conditions: ultra-sonicated CN_x (3.2 mg), co-catalyst, pre-treated PET (50 mg), aq. KOH (1 M, 2 mL), sealed photoreactor (internal volume 7.91 mL) under anaerobic conditions, simulated solar light (AM 1.5G, 100 mW cm^{-2}, 25 °C). Yields are cumulative values. σ is the standard deviation calculated from 3 samples.

Co-catalyst	Time (h)	Yield ± σ ($\mu mol_{H_2}\ g_{sub}^{-1}$)	Activity ± σ ($\mu mol_{H_2}\ g_{cat}^{-1}\ h^{-1}$)
Ni, 5 wt% (Ni(NO$_3$)$_2$·6H$_2$O)[a]	4	0.0 ± 0.0	0.0 ± 0.0
	20	11.8 ± 2.5	9.19 ± 1.96
Ni, 5 wt% (Ni(BF$_4$)$_2$·6H$_2$O)[a,b]	4	0.00	0.00
	20	9.34	7.30
Ni, 2 wt% (Ni(acac$_2$)$_3$)[c]	4	0.0 ± 0.0	0.0 ± 0.0
	20	9.44 ± 0.49	7.37 ± 0.38
NiO, 5 wt%[d]	4	0.0 ± 0.0	0.0 ± 0.0
	20	0.0 ± 0.0	0.0 ± 0.0
NiO NPs, 5 wt%[d]	4	0.0 ± 0.0	0.0 ± 0.0
	20	0.0 ± 0.0	0.0 ± 0.0
Ni(OH)$_2$, 5 wt%[e]	4	0.0 ± 0.0	0.0 ± 0.0
	20	16.5 ± 2.3	12.9 ± 1.80
Ni$_2$P, 2 wt%	4	5.06 ± 0.34	19.8 ± 1.3
	20	27.6 ± 3.4	21.6 ± 2.7
Fe, 5 wt% (Fe(NO$_3$)$_3$·9H$_2$O)[a]	4	0.0 ± 0.0	0.0 ± 0.0
	20	0.0 ± 0.0	0.0 ± 0.0
Fe, 5 wt% (Fe(BF$_4$)$_2$·6H$_2$O)[a,b]	4	0.0	0.0
	20	1.76	1.37
Fe$_2$O$_3$, 5 wt%[d]	4	0.0 ± 0.0	0.0 ± 0.0
	20	0.0 ± 0.0	0.0 ± 0.0
Fe$_3$O$_4$ NPs, 5 wt%[d]	4	0.0 ± 0.0	0.0 ± 0.0
	20	0.933 ± 0.144	0.729 ± 0.112
Fe$_x$P, 2 wt%[a,f]	4	0.0	0.0
	20	0.620	0.484
CuO NPs, 5 wt%[d]	4	0.0 ± 0.0	0.0 ± 0.0
	20	0.0 ± 0.0	0.0 ± 0.0
Co, 5 wt% (Co(BF$_4$)$_2$·6H$_2$O)[a,b]	4	0.00	0.00
	20	4.54	2.95

[a] Metal salts were simply dissolved in H_2O and added to CN_x.

[b] Single run measurements.

[c] CN_x|Ni was synthesized as previously reported.[5] Ni(II) acetylacetone (11 mg) and CN_x (150 mg) were mixed in a minimum of water and stirred and sonicated for 1 h each. After drying under vacuum at 60 °C, the powder was heated for 1 h at 200 °C under Ar (ramp rate 5 °C min^{-1}). The solid was cooled, washed with water (3×) and ethanol (3×), and dried under vacuum.

[d] Metal oxides were ground with CN_x with a pestle and mortar.

[e] A literature procedure was modified slightly.[11] CN_x (40 mg), Ni(NO$_3$)$_2$·6H$_2$O (5 mg) and 0.05 M NaOH (10 mL) were combined and stirred for 20 h. The mixture was centrifuged at 7000 rpm for 5 min. The precipitate was then washed with water (3×) and ethanol (3×), and dried under vacuum.

[f] The Ni$_2$P synthesis procedure was adapted to produce CN_x|Fe$_x$P. FeCl$_3$·6H$_2$O (10 mg), NaH$_2$PO$_2$·H$_2$O (50 mg), and CN_x (150 mg) were mixed in a minimum of water, stirred for 1 h and sonicated for 1 h. The mixture was dried under vacuum at 60 °C and heated for 1 h at 200 °C under Ar (ramp rate 5 °C min^{-1}). After cooling, the powder was washed with water (3×) and ethanol (3×), and dried under vacuum.

Table S10. Photoreforming of a variety of substrates with $CN_x|Ni_2P$. Conditions: ultra-sonicated $CN_x|Ni_2P$ 2 wt% (3.2 mg), pre-treated polymer (50 mg), aq. KOH (1 M, 2 mL), sealed photoreactor (internal volume 7.91 mL) under anaerobic conditions, simulated solar light (AM 1.5G, 100 mW cm^{-2}, 25 °C). Yields and activities are cumulative values. Single measurements only.

Substrate	Time (h)	Yield (μmol_{H_2} g_{sub}^{-1})	Activity (μmol_{H_2} g_{cat}^{-1} h^{-1})
PE	4	1.76	6.87
	20	6.88	5.37
PET	4	3.62	14.1
	20	39.9	31.2
PLA	4	4.22	16.5
	20	42.1	32.9
PP	4	1.74	6.80
	20	7.72	6.03
PS	4	2.32	9.06
	20	6.14	4.80
PUR	4	1.22	4.76
	20	7.74	6.05
Rubber	4	1.54	6.01
	20	5.56	4.34

Table S11. Photoreforming of PET and PLA with $CN_x|Ni_2P$. Conditions: ultra-sonicated $CN_x|Ni_2P$ 2 wt% (3.2 mg), pre-treated polymer (50 mg), aq. KOH (1 M, 2 mL), sealed photoreactor (internal volume 7.91 mL) under anaerobic conditions, simulated solar light (AM 1.5G, 100 mW cm^{-2}, 25 °C). Yields and activities are cumulative values. σ is the standard deviation calculated from 3 samples.

Description	Time (h)	Yield ± σ (μmol_{H_2} g_{sub}^{-1})	Activity ± σ (μmol_{H_2} g_{cat}^{-1} h^{-1})
Long-term photoreforming of pre-treated PET	2	3.90 ± 0.19	30.5 ± 1.5
	4	6.52 ± 0.33	25.5 ± 1.3
	20	33.1 ± 1.7	25.8 ± 1.3
	25	42.1 ± 3.4	26.3 ± 2.1
	27	45.4 ± 2.3	26.3 ± 1.3
	44	72.0 ± 6.9	25.6 ± 2.5
	46	73.5 ± 7.5	25.0 ± 2.5
	50	82.5 ± 7.3	25.7 ± 2.3
Long-term photoreforming of pre-treated PLA	2	5.50 ± 0.27	43.0 ± 2.1
	4	9.92 ± 0.50	38.7 ± 1.9
	20	59.7 ± 6.0	46.6 ± 4.7
	25	77.8 ± 6.8	48.6 ± 4.3
	27	86.4 ± 6.4	50.0 ± 3.7
	44	156 ± 12	55.4 ± 4.2
	46	164 ± 15	55.8 ± 5.1
	50	178 ± 12	55.7 ± 3.7

Table S12. External quantum yield (EQY) measurements from photoreforming of polymers. Conditions: ultra-sonicated $CN_x|Ni_2P$ 2 wt% (3.2 mg), pre-treated polymer (50 mg), aq. KOH (1 M, 2 mL), all in a sealed quartz cuvette (path length 1 cm, internal volume 3.83 mL) under anaerobic conditions. Samples were irradiated with monochromatic light (λ = 430 nm, full-width at half maximum: 5, intensity taken as the average of the intensities measured at the beginning and end of the experiments) over an area of 0.28 cm². σ is the standard deviation calculated from the 3 listed samples.

Substrate	Substrate Conditions	Time (h)	Light Intensity (mW cm^{-2})	H$_2$ (µmol)	EQY (%)	Average ± σ EQY (%)
PLA	25 mg mL^{-1}, pre-treated	24	0.64 ± 0.10	0.022	0.078	0.101 ± 0.018
			0.95 ± 0.07	0.043	0.097	
			0.90 ± 0.01	0.052	0.128	
PET	25 mg mL^{-1}, pre-treated	24	0.50 ± 0.08	0.009	0.041	0.035 ± 0.005
			0.75 ± 011	0.009	0.028	
			0.90 ± 0.01	0.014	0.036	

Table S13. Stoichiometric H$_2$ conversion calculations. Conditions: ultra-sonicated $CN_x|Ni_2P$ 2 wt% (3.2 mg), polymer (5 mg), aq. KOH (1 M or 10 M, 2 mL), sealed photoreactor (internal volume 7.91 mL) under anaerobic conditions, simulated solar light (AM 1.5G, 100 mW cm^{-2}, 25 °C). Yields and activities are cumulative values. σ is the standard deviation calculated from 3 samples.

Description	Substrate	$N_{100\%}$ (mol$_{H_2}$ mol$_{sub}$$^{-1}$)	Time (h)	N_{yield} ± σ (mol$_{H_2}$ mol$_{sub}$$^{-1}$)	Conversion ± σ (%)
H$_2$ Conversion in 1 M KOH	PET, 26.0 µmol	5.0[a]	72	0.027 ± 0.003	0.54 ± 0.06
			96	0.040 ± 0.004	0.80 ± 0.08
			144	0.121 ± 0.015	2.42 ± 0.30
			192	0.219 ± 0.029	4.38 ± 0.58
	PLA, 69.4 µmol	6.0	72	0.016 ± 0.002	0.27 ± 0.03
			96	0.026 ± 0.004	0.43 ± 0.07
			144	0.061 ± 0.012	1.02 ± 0.20
			192	0.097 ± 0.015	1.62 ± 0.25
H$_2$ Conversion in 10 M KOH	PET, 26.0 µmol	5.0[a]	72	0.284 ± 0.014	5.68 ± 0.28
			96	0.385 ± 0.037	7.70 ± 0.74
			144	0.932 ± 0.114	18.6 ± 2.3
			192	1.23 ± 0.16	24.5 ± 3.3
	PLA, 69.4 µmol	6.0	72	0.079 ± 0.005	1.32 ± 0.08
			96	0.135 ± 0.012	2.25 ± 0.20
			144	0.295 ± 0.033	4.92 ± 0.55
			192	0.401 ± 0.048	6.68 ± 0.80

[a] This number assumes that only the ethylene glycol component of PET is oxidized.

Table S14. Photoreforming with other photocatalysts. $CN_x|Ni_2P$ is included for ease of comparison. Conditions: catalyst (3.2 mg), pre-treated polymer (50 mg), aq. KOH (1 M, 2 mL), sealed photoreactor (internal volume 7.91 mL) under anaerobic conditions, simulated solar light (AM 1.5G, 100 mW cm^{-2}, 25 °C). Yields and activities are cumulative values. σ is the standard deviation calculated from 3 samples.

Description	Catalyst	Substrate	Time (h)	Yield ± σ ($\mu mol_{H_2}\ g_{sub}^{-1}$)	Activity ± σ ($\mu mol_{H_2}\ g_{cat}^{-1}\ h^{-1}$)
	$CN_x|Ni_2P$, 2 wt%	PET	4	6.52 ± 0.33	25.5 ± 1.3
			20	33.1 ± 1.7	25.8 ± 1.3
			25	42.1 ± 3.4	26.3 ± 2.1
			44	72.0 ± 6.9	25.6 ± 2.5
		PLA	4	9.92 ± 0.50	38.7 ± 1.9
			20	59.7 ± 6.0	46.6 ± 4.7
			25	77.8 ± 6.8	48.6 ± 4.3
			44	156 ± 12	55.4 ± 4.2
Alternative photocatalysts	2 wt% Ni_2P powder + CN_x	PET	4	0.24 ± 0.013	0.937 ± 0.051
			20	10.5 ± 0.7	8.22 ± 0.55
	$^{H_2N}CN_x|Ni_2P$, 2 wt%	PET	4	10.5 ± 2.1	41.1 ± 8.2
			20	34.3 ± 3.1	26.8 ± 2.4
			25	39.5 ± 3.2	24.7 ± 2.0
			44	42.5 ± 5.5	15.1 ± 2.0
		PLA	4	21.1 ± 2.8	82.5 ± 10.9
			20	81.2 ± 6.1	63.4 ± 4.7
			25	98.6 ± 7.8	61.6 ± 4.8
			44	141 ± 18	50.2 ± 6.4
	$TiO_2|Ni_2P$, 2 wt%	PET	4	0.900 ± 0.105	3.52 ± 0.41
			20	13.8 ± 2.4	10.8 ± 1.9
		PLA	4	8.48 ± 5.12	33.1 ± 20.0
			20	54.1 ± 9.4	42.3 ± 7.4
	$CN_x|Pt$, 2 wt%	PET	4	29.7 ± 6.1	116 ± 24
			20	96.2 ± 4.8	75.2 ± 3.7
		PLA	4	20.0 ± 1.3	156 ± 10
			20	180 ± 17	281 ± 26
	CN_x-P|Pt, 2 wt%	PET	4	16.5 ± 0.8	64.5 ± 3.2
			20	92.6 ± 11.5	72.4 ± 9.0
Alternative photocatalyst irradiated with λ > 420 nm filter	$TiO_2|Ni_2P$, 2 wt%	PET	4	0.0 ± 0.0	0.0 ± 0.0
			20	0.0 ± 0.0	0.0 ± 0.0
		PLA	4	0.0 ± 0.0	0.0 ± 0.0
			20	0.0 ± 0.0	0.0 ± 0.0
	$^{H_2N}CN_x|Ni_2P$, 2 wt%	PET	4	0.0 ± 0.0	0.0 ± 0.0
			20	0.720 ± 0.480	0.562 ± 0.374
		PLA	4	0.320 ± 0.016	0.205 ± 0.010
			20	7.20 ± 0.36	3.25 ± 0.30

Table S15. Comparison of the current work to other reported catalysts for polymer photoreforming. Samples referenced as [12] were irradiated with a 500 W Xe lamp. Samples referenced as * or [13] were irradiated with a 1000 W Xe lamp (AM 1.5G, 100 mW cm^{-2}, 25 °C).

Catalyst	Substrate[a]	[base][b]	Time (h)	Yield ± σ (μmol_{H_2} g_{sub}^{-1})	Activity ± σ (μmol_{H_2} g_{cat}^{-1} h^{-1})	Ref
TiO$_2$|Pt, 5%[c,d]	PE	5 M	10	620	31.0	12
TiO$_2$|Pt, 5%	PVC	5 M	10	300	28.7	12
TiO$_2$|Pt, 5%	PET	10 M	20	1220 ± 110	153 ± 14	13
CdS/CdO$_x$[e]	PET	10 M	20	460 ± 58	4810 ± 600	13
H$_2$NCN$_x$|Ni$_2$P, 2%[f]	PET	10 M	20	141 ± 16	110 ± 12	*
TiO$_2$|Ni$_2$P, 2%	PET	10 M	20	119 ± 8	93.0 ± 6.6	*
CN$_x$|Ni$_2$P, 2%	PET	10 M	20	111 ± 8	83.2 ± 6.0	*
CN$_x$|Pt, 2%	PET	10 M	20	104 ± 4	81.1 ± 3.4	*
CdS/CdO$_x$	PET	1 M	20	132 ± 6	2210 ± 110	13
CN$_x$|Pt, 2%	PET	1 M	20	96.2 ± 4.8	75.2 ± 3.7	*
H$_2$NCN$_x$|Ni$_2$P, 2%	PET	1 M	20	34.3 ± 3.1	26.8 ± 2.4	*
CN$_x$|Ni$_2$P, 2%	PET	1 M	20	33.1 ± 1.7	25.8 ± 1.3	*
TiO$_2$|Ni$_2$P, 2%[f]	PET	1 M	20	13.8 ± 2.4	10.8 ± 1.9	*
CdS/CdO$_x$	PLA	10 M	20	2590 ± 690	63000 ± 16800	13
H$_2$NCN$_x$|Ni$_2$P, 2%	PLA	10 M	20	427 ± 21	333 ± 17	*
TiO$_2$|Pt, 5%	PLA	10 M	20	358 ± 53	89 ± 13	13
CN$_x$|Pt, 2%	PLA	10 M	20	314 ± 16	491 ± 24	*
TiO$_2$|Ni$_2$P, 2%	PLA	10 M	20	220 ± 28	173 ± 22	*
CN$_x$|Ni$_2$P, 2%	PLA	10 M	20	211 ± 10	165 ± 8	*
CN$_x$|Pt, 2%	PLA	1 M	20	180 ± 17	281 ± 26	*
H$_2$NCN$_x$|Ni$_2$P, 2%	PLA	1 M	20	81.2 ± 6.1	63.4 ± 4.8	*
CN$_x$|Ni$_2$P, 2%	PLA	1 M	20	59.7 ± 6.0	46.6 ± 4.7	*
CdS/CdO$_x$	PLA	1 M	20	56.6 ± 8.9	839 ± 132	13
TiO$_2$|Ni$_2$P, 2%	PLA	1 M	20	54.1 ± 9.4	42.3 ± 7.4	*

[a] All polymer substrates *except* for PE and PVC were pre-treated prior to use (25 mg mL^{-1}).

[b] PE and PVC were run in 30 mL of base, whereas all other samples were run in 2 mL of base.

[c] Percentages indicate wt% of the co-catalyst.

[d] 300 mg TiO$_2$\|Pt used per sample.

[e] 1 nmol CdS/CdO$_x$ used per sample.

[f] 3.2 mg H$_2$NCN$_x$\|Ni$_2$P, CN$_x$\|Ni$_2$P, CN$_x$\|Pt or TiO$_2$\|Ni$_2$P used per sample.

* This work.

Table S16. Photoreforming of oxidation intermediates with CN$_x$|Ni$_2$P. Conditions: CN$_x$|Ni$_2$P 2 wt% (3.2 mg), substrate (50 mg), aq. KOH (1 M, 2 mL), sealed photoreactor (internal volume 7.91 mL) under anaerobic conditions, simulated solar light (AM 1.5G, 100 mW cm^{-2}, 25 °C). Yields and activities are cumulative values. σ is the standard deviation calculated from 3 samples, unless stated otherwise.

Substrate	Time (h)	Yield $\pm \sigma$ (μmol_{H_2} g$_{sub}^{-1}$)	Activity $\pm \sigma$ (μmol_{H_2} g$_{cat}^{-1}$ h^{-1})
Acetate[a]	4	1.12 ± 0.14	4.37 ± 0.56
	20	3.22 ± 0.40	2.51 ± 0.31
Ethylene glycol	4	12.9 ± 0.6	50.5 ± 2.5
	20	58.9 ± 7.1	46.0 ± 5.6
Formate[a]	4	4.30 ± 1.80	16.8 ± 7.0
	20	17.7 ± 1.3	13.8 ± 1.0
Glycolate[a]	4	3.58 ± 0.85	14.0 ± 3.32
	20	14.6 ± 2.1	11.4 ± 1.7
Glyoxal[a]	4	10.6 ± 0.5	41.3 ± 2.1
	20	50.2 ± 6.2	39.2 ± 4.9
Lactate	4	6.20 ± 0.77	24.2 ± 3.0
	20	40.4 ± 3.4	31.6 ± 2.7
Terephthalate	4	0.0 ± 0.0	0.0 ± 0.0
	20	0.0 ± 0.0	0.0 ± 0.0

[a] σ obtained from two samples.

Table S17. Re-use of CN$_x$|Ni$_2$P for photoreforming of PET. Conditions: previously used CN$_x$|Ni$_2$P 2 wt% after centrifugation, washing and drying (3.2 mg), pre-treated PET (50 mg), aq. KOH (1 M, 2 mL), sealed photoreactor (internal volume 7.91 mL) under anaerobic conditions, simulated solar light (AM 1.5G, 100 mW cm^{-2}, 25 °C). Yields and activities are cumulative values. σ is the standard deviation calculated from 3 samples.

Time (h)	Yield $\pm \sigma$ (μmol_{H_2} g$_{sub}^{-1}$)	Activity $\pm \sigma$ (μmol_{H_2} g$_{cat}^{-1}$ h^{-1})
4	0.60 ± 0.03	2.34 ± 0.12
20	14.6 ± 0.7	11.4 ± 0.6

Table S18. Quantification of the organic oxidation products formed from glyoxal and formate after 24 h of photoreforming. Maleic acid in D$_2$O was used as an internal standard.

	Organic compound	Quantity (nmol)
Photoreforming of glyoxal	Acetate	260
	Formate	1640
	Glycolate	6550
Photoreforming of formate	Acetate	115

Table S19. Photoreforming of different quantities of polyester microfibers. Conditions: $CN_x|Ni_2P$ 2 wt% (3.2 mg), pre-treated fibers, aqueous KOH (1 M, 2 mL), sealed photoreactor (internal volume 7.91 mL) under anaerobic conditions, simulated solar light (AM 1.5G, 100 mW cm^{-2}, 25 °C). Yields and activities are cumulative values. Single measurements only.
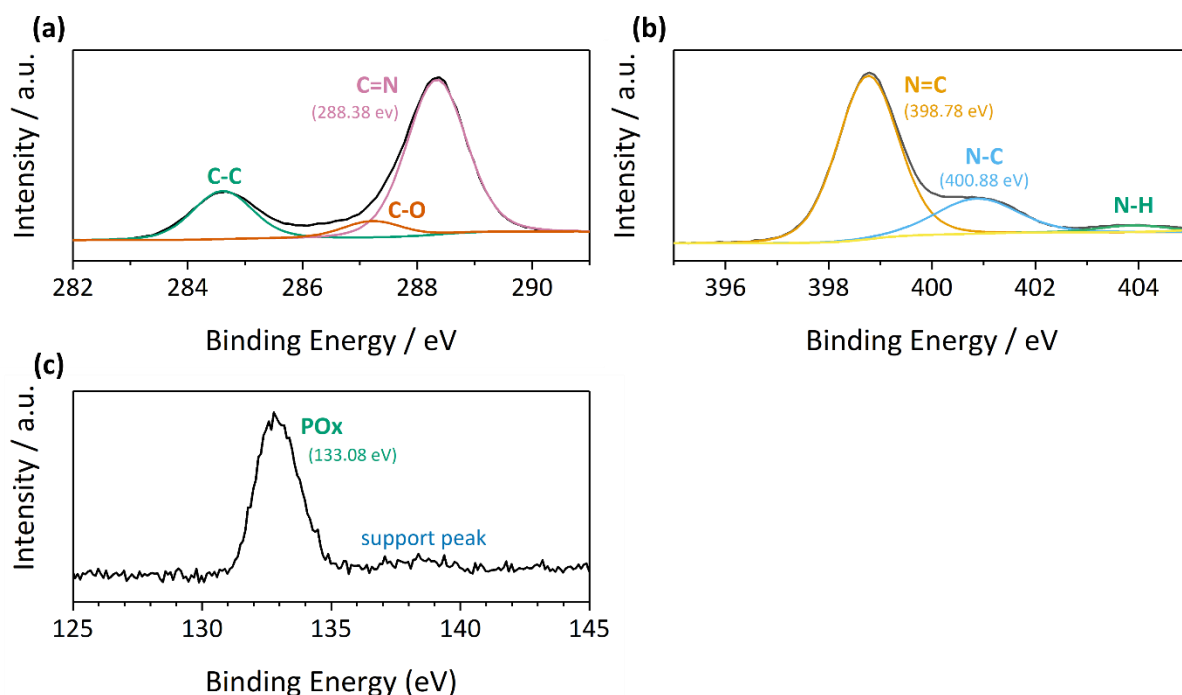
Substrate Concentration (mg mL^{-1})	Time (h)	Yield (μmol_{H_2} g_{sub}^{-1})	Activity (μmol_{H_2} g_{cat}^{-1} h^{-1})
2.5	4	0.0	0.0
	20	0.0	0.0
0.5	4	0.0	0.0
	20	0.0	0.0
0.25	4	0.0	0.0
	20	0.0	0.0

Table S20. Long-term photoreforming of real-world waste at small and large scales. Conditions: $CN_x|Ni_2P$ 2 wt% (3.2 mg for small scale, or 170 mg for up-scaled), pre-treated polymer (5 mg mL^{-1} microfibers, 25 mg mL^{-1} bottle, 5 mg mL^{-1} oil), aq. KOH (1 M, 2 mL for small scale, or 120 mL for up-scaled), sealed photoreactor (internal volume 7.91 mL for small scale, 190 mL for up-scaled) under anaerobic conditions, simulated solar light (AM 1.5G, 100 mW cm^{-2}, 25 °C). Yields and activities are cumulative values. σ is the standard deviation calculated from 3 samples.

Description	Time (h)	Yield ± σ (μmol_{H_2} g_{sub}^{-1})	Activity ± σ (μmol_{H_2} g_{cat}^{-1} h^{-1})
Long-term photoreforming of pre-treated microfibers	24	17.6 ± 2.3	2.29 ± 0.30
	48	31.2 ± 3.5	2.03 ± 0.23
	72	43.4 ± 2.9	1.88 ± 0.12
	96	63.3 ± 4.4	2.06 ± 0.14
	120	104 ± 10	2.67 ± 0.25
Long-term photoreforming of pre-treated bottle	24	4.38 ± 0.54	2.85 ± 0.35
	48	8.64 ± 0.43	2.81 ± 0.14
	72	11.6 ± 0.5	2.52 ± 0.12
	96	16.1 ± 1.0	2.61 ± 0.17
	120	22.0 ± 1.3	2.87 ± 0.16
Long-term photoreforming of pre-treated bottle + oil	24	2.40 ± 0.16	1.87 ± 0.12
	48	5.23 ± 1.08	2.04 ± 0.42
	72	6.47 ± 0.32	1.68 ± 0.08
	96	8.27 ± 0.55	1.61 ± 0.11
	120	11.4 ± 1.2	1.78 ± 0.19
Up-scaled photoreforming of pre-treated microfibers[a]	24	18.3	2.69
	48	28.5	2.09
	72	37.7	1.85
	96	46.1	1.69
	120	53.5	1.57

[a] Values from a single experiment.

Supplementary Figures

Figure S1. X-ray photoelectron spectroscopy (XPS) spectra of the **(a)** C_{1s}, **(b)** N_{1s}, and **(c)** P_{2p} edges of CN_x-P. CN_x-P was produced according to the same synthesis procedure utilized for $CN_x|Ni_2P$, but without the addition of the Ni precursor. These data (along with ICP results in Table S1), suggest that excess P content in the $CN_x|Ni_2P$ photocatalyst can be attributed to residual PO_x from the co-catalyst synthesis that adheres to the CN_x surface.
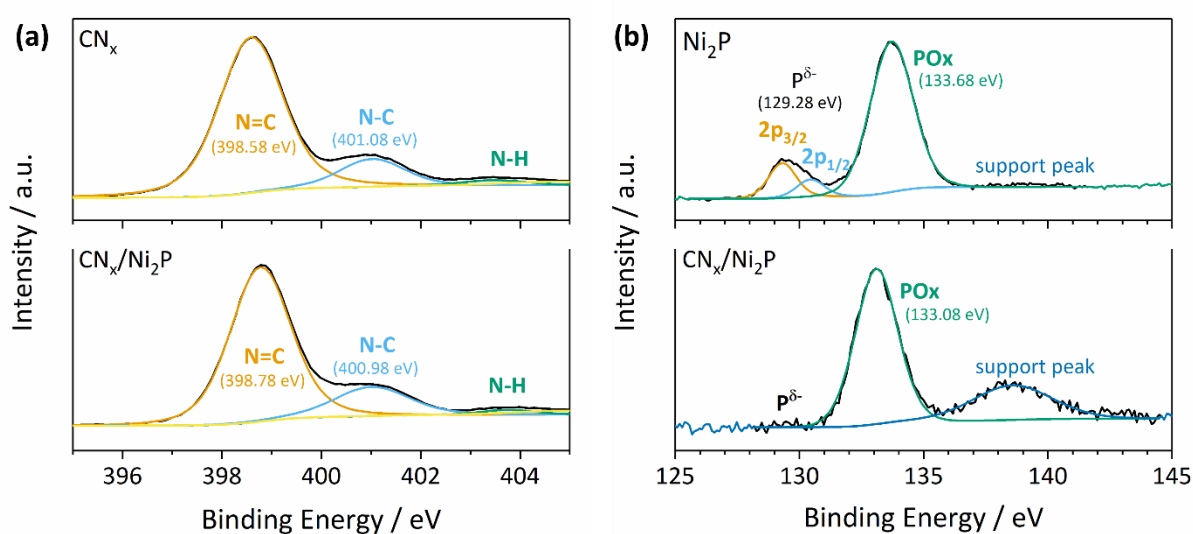
Figure S2. X-ray photoelectron spectroscopy (XPS) spectra of the **(a)** N_{1s} edge of CN_x and $CN_x|Ni_2P$ (2 wt%), and **(b)** P_{2p} edge of Ni_2P and $CN_x|Ni_2P$ (2 wt%).
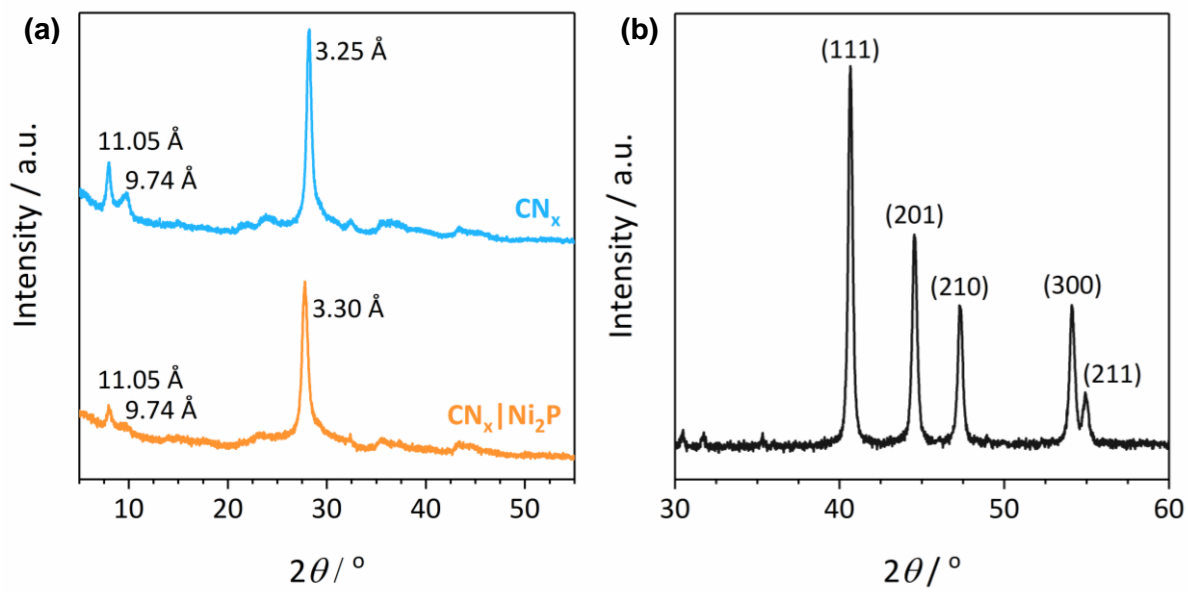
Figure S3. Powder X-ray diffraction (XRD) patterns of **(a)** CN_x and $CN_x|Ni_2P$ (2 wt%) and **(b)** Ni_2P.
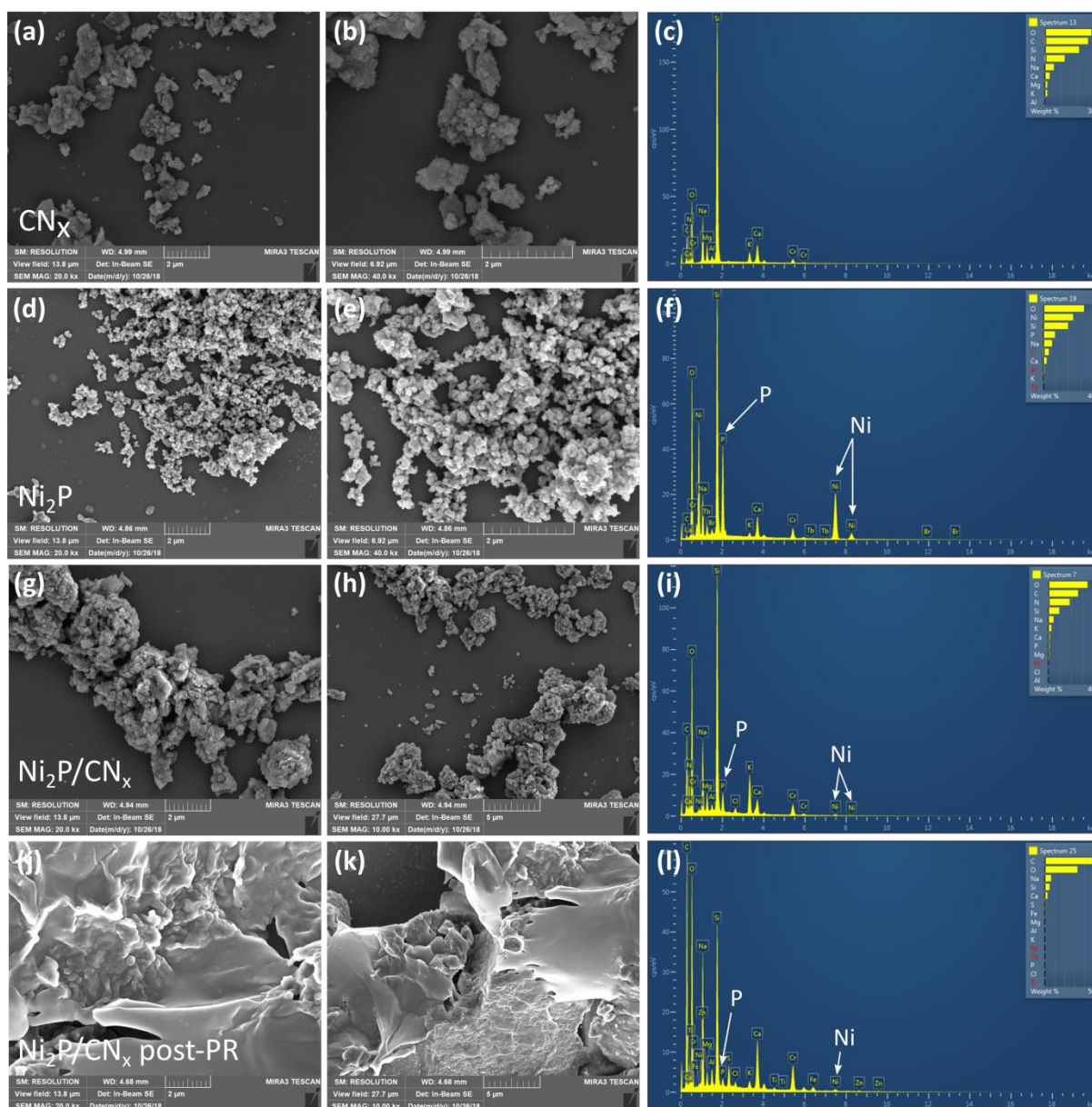
Figure S4. Scanning electron microscopy (SEM) images and energy dispersive X-ray spectroscopy (EDX) spectra of **(a-c)** CN_x, **(d-f)** Ni_2P, **(g-i)** $CN_x|Ni_2P$ (2 wt%), and **(j-l)** $CN_x|Ni_2P$ (2 wt%) after photoreforming. Samples were sputtered with 10 nm of Cr prior to imaging. Photoreforming conditions: $CN_x|Ni_2P$ (3.2 mg), PLA (50 mg), 1 M aqueous KOH (2 mL), simulated solar irradiation (AM 1.5G, 100 mW cm^{-2}, 25 °C, 50 h).
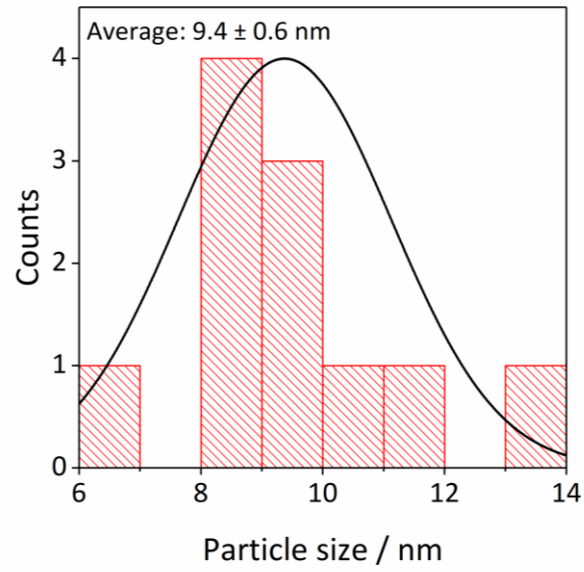
Figure S5. Particle size analysis of Ni_2P nanoparticles annealed with CN_x, as measured from transmission electron microscopy (TEM) images.
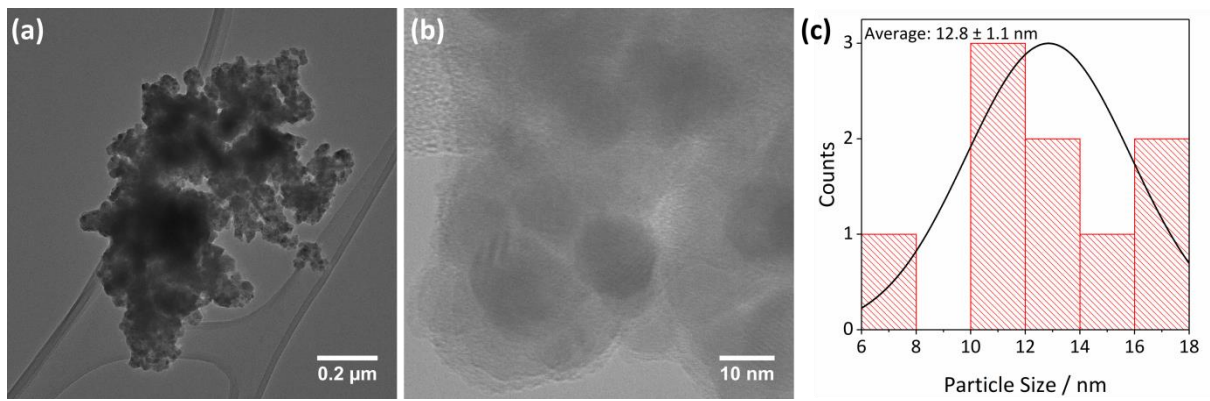
Figure S6. **(a-b)** TEM images of Ni_2P nanoparticles. **(c)** Particle size analysis of the Ni_2P nanoparticles.
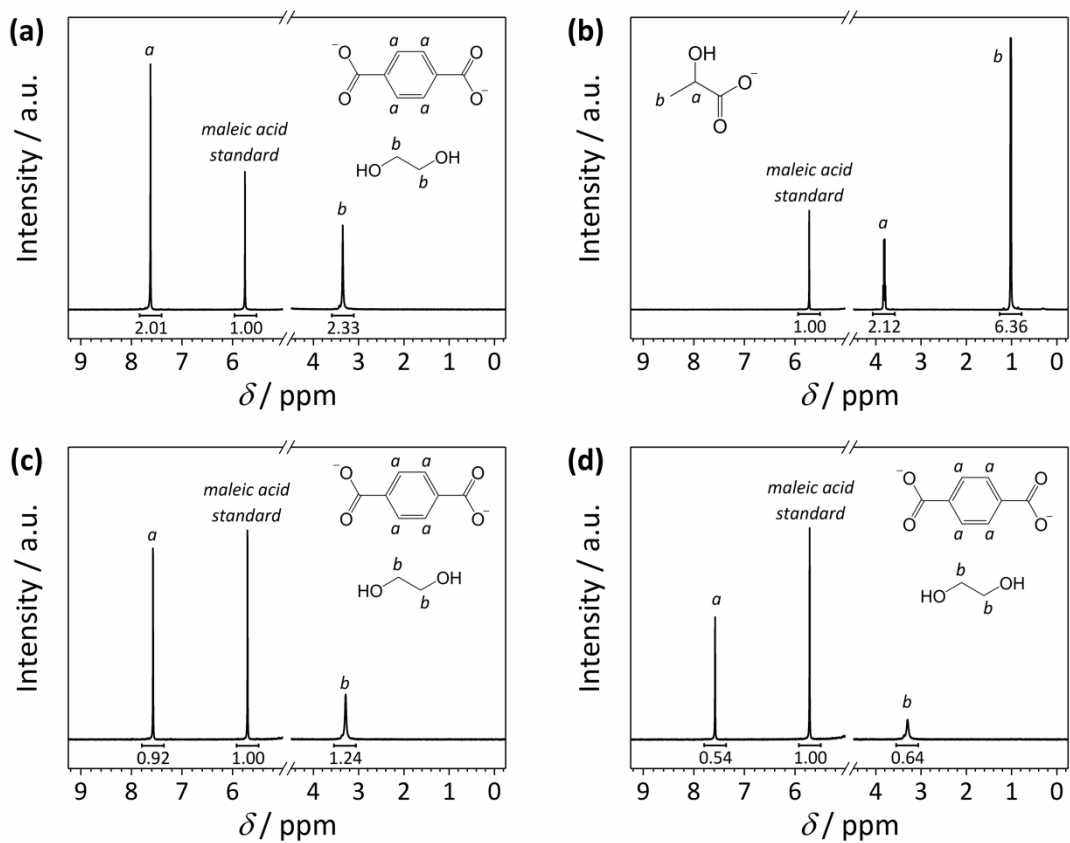
Figure S7. ^{1}H-NMR quantification of polymer solubilisation after pre-treatment. **(a)** PET, **(b)** PLA, **(c)** PET bottle and **(d)** polyester microfiber in 1 M NaOD in D_2O with maleic acid as a standard.
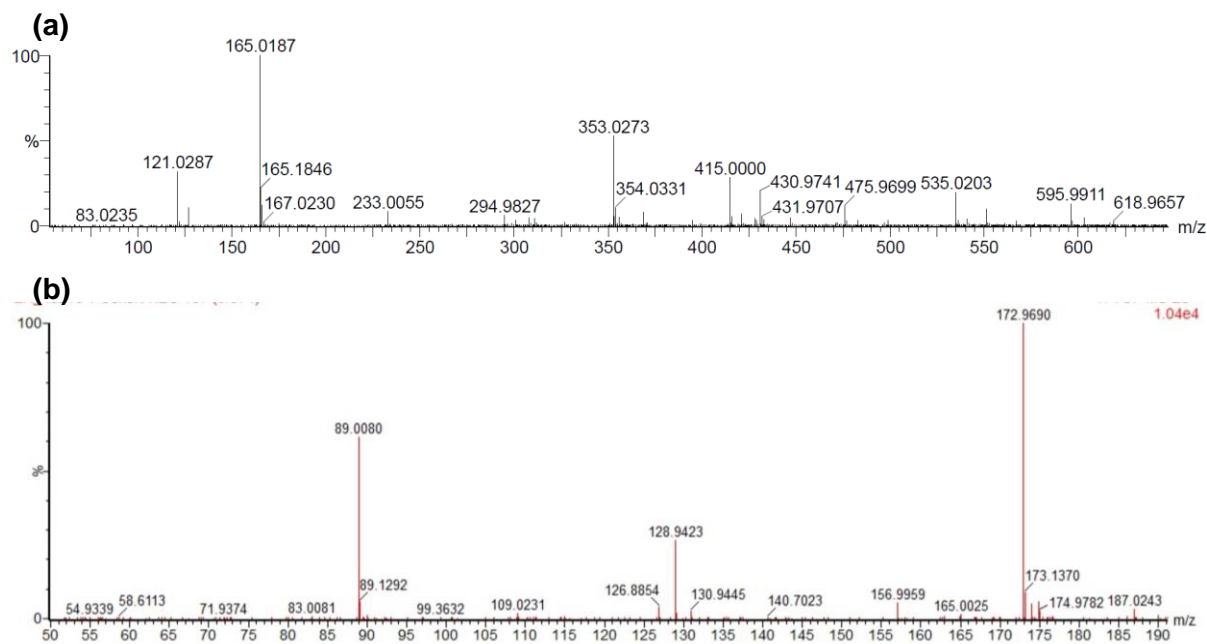
Figure S8. Liquid chromatography-mass spectrometry (LC-MS, negative ion mode) of solubilized **(a)** PET and **(b)** PLA components after pre-treatment. Samples were hydrolysed in 1 M aq. KOH and then diluted with methanol to 0.01 M KOH for analysis, with measurements recorded up to 1000 m/z. In **(a)**, The peak at 165 m/z corresponds to terephthalate and the peak at 121 m/z is a fragment of terephthalate (benzoate); no peaks are observed for common PET hydrolysis products such as mono(2-hydroxyethyl) terephthalate (MHET, 210 g mol^{-1}) or bis(2-hydroxyethyl) terephthalate (BHET, 254 g mol^{-1}), but peaks at 121, 353, 451, etc. m/z may be from oligomer fragments. In **(b)**, the peak at 89 m/z corresponds to lactate, while the peaks at 129 and 173 m/z are likely oligomer fragments.
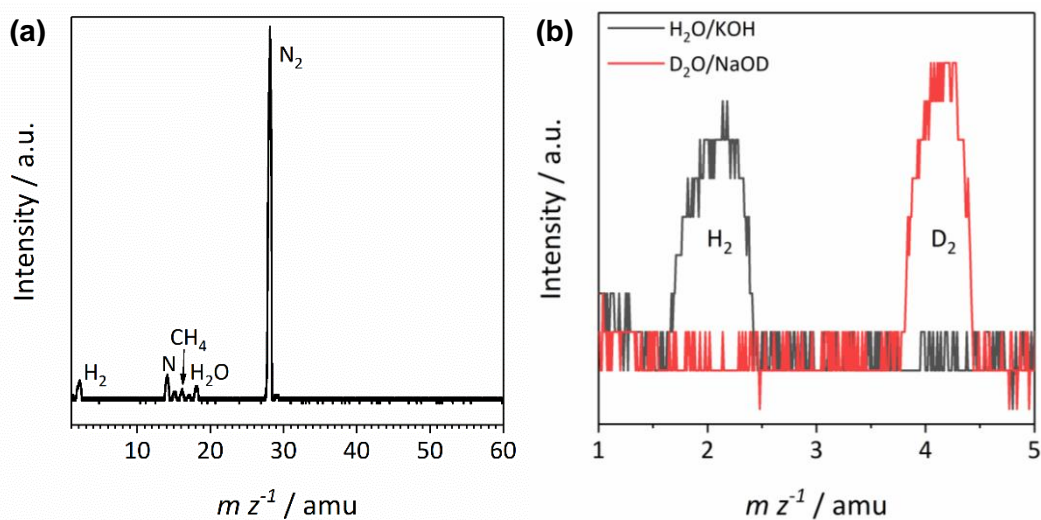
Figure S9. Mass spectra of the gas evolved after photoreforming (AM 1.5G, 100 mW cm^{-2}, 72 h) of PET (25 mg mL^{-1}) over CN$_x$|Ni$_2$P (3.2 mg) in **(a)** 1 M aq. KOH and **(b)** 1 M aq. KOH or 1 M NaOD in D$_2$O (2 mL).
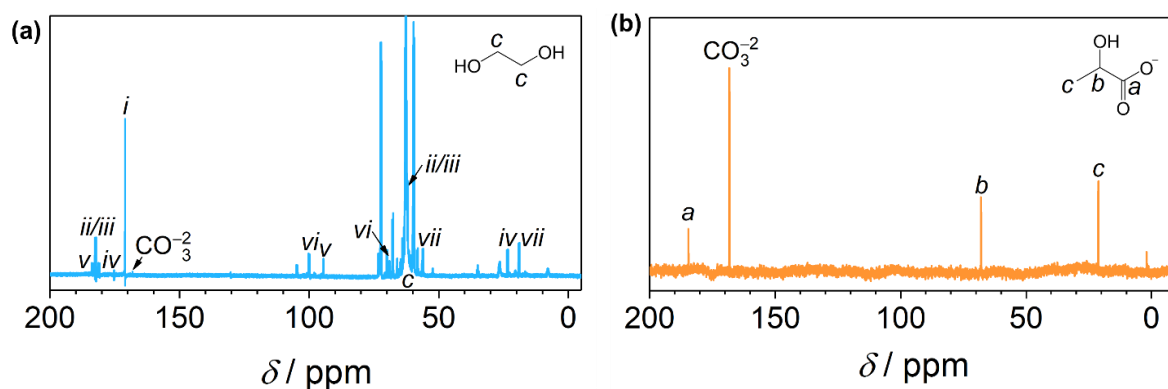
**Figure S10**. ^{13}C-NMR spectrum of **(a)** ^{13}C-labelled ethylene glycol (100 mg) and **(b)** PLA (3 mg) after photoreforming (AM 1.5G, 100 mW cm^{-2}, 25 °C, 5 days) over CN$_x$|Ni$_2$P 2 wt% (3.2 mg) in 1 M NaOD in D$_2$O (2 mL). The labels are attributed as follows: *(i)* formate, *(ii)* glyoxal, *(iii)* glycolate, *(iv)* acetate, *(v)* glyoxylate, *(vi)* glycoaldehyde, *(vii)* ethanol.
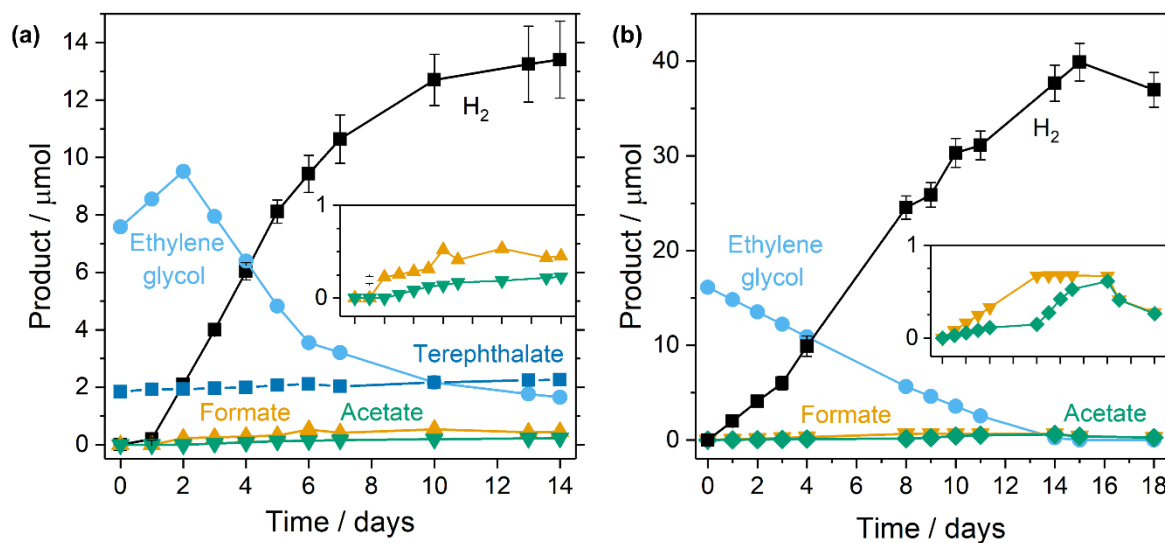
Figure S11. Long-term photoreforming of **(a)** PET (3 mg) and **(b)** ethylene glycol (1 mg) over $CN_x|Ni_2P$ (1.6 mg mL^{-1}). Conditions: 5 M aq. KOH or 5 M NaOD in D_2O (2 mL), simulated sunlight (AM 1.5G, 100 mW cm^{-2}, 25 °C). Aqueous products were analyzed using ^{1}H-NMR with maleic acid as an internal standard. Insets show a zoomed-in view of the formate and acetate curves. The observed mass imbalance is due to unidentified oxidation products.
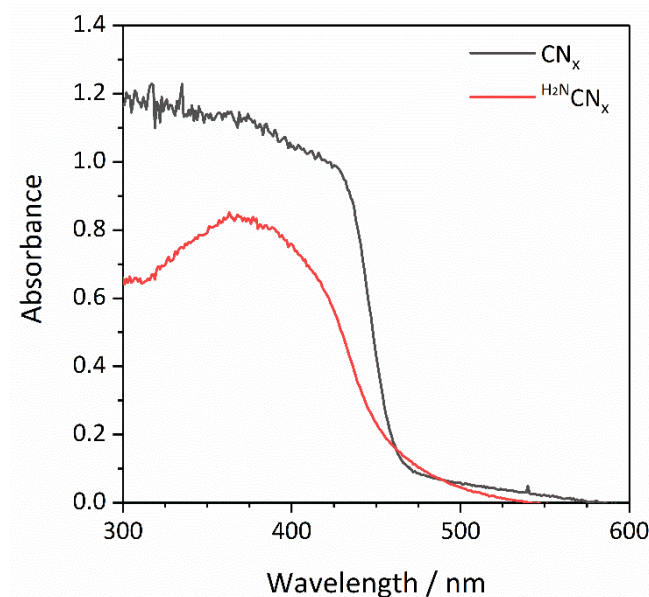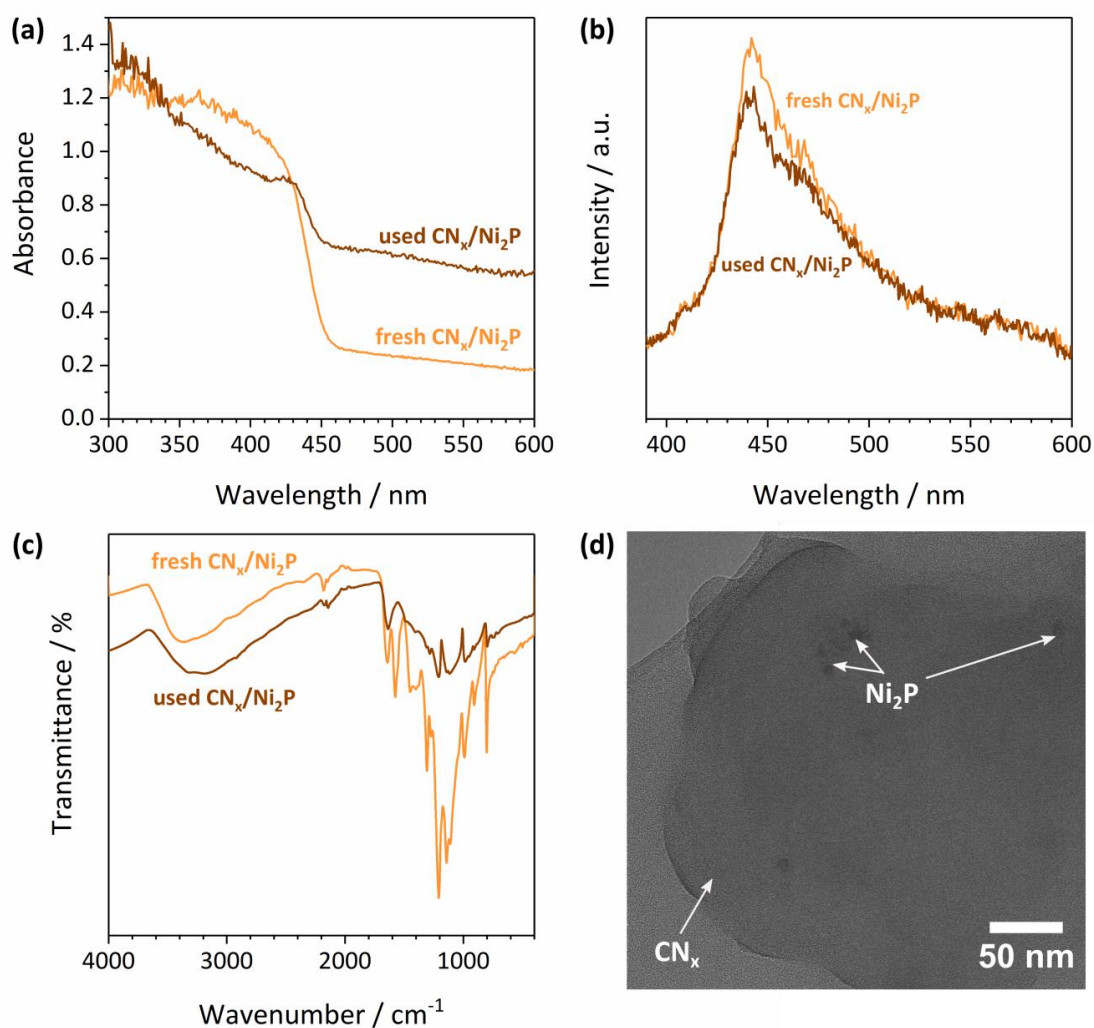

Figure S12. Comparison of the diffuse reflectance UV-Vis spectra of CN_x and $^{H2N}CN_x$.
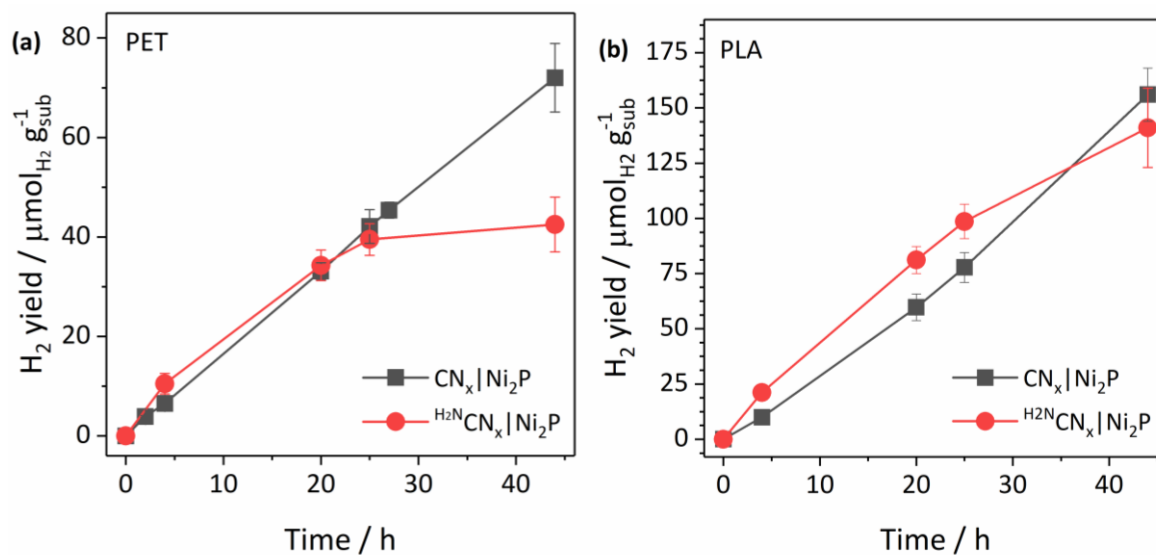
**Figure S13**. Comparison of photoreforming of **(a)** PET and **(b)** PLA over $CN_x|Ni_2P$ and $^{H_2N}CN_x|Ni_2P$. Conditions: photocatalyst (3.2 mg), pre-treated polymer (25 mg mL^{-1}), aqueous KOH (1 M, 2 mL), irradiation (AM 1.5G, 100 mW cm^{-2}, 25 °C).

S23

Figure S14. Post-photoreforming characterization of the CN$_x$|Ni$_2$P (2 wt%) photocatalyst. **(a)** UV-Vis, **(b)** emission (λ_{ex} = 360 nm, λ_{em} = 450 nm), and **(c)** FTIR spectra. **(d)** TEM image. Photoreforming conditions: CN$_x$|Ni$_2$P (3.2 mg), PLA (50 mg), 1 M aqueous KOH (2 mL), simulated solar irradiation (AM 1.5G, 100 mW cm^{-2}, 25 °C, 50 h).
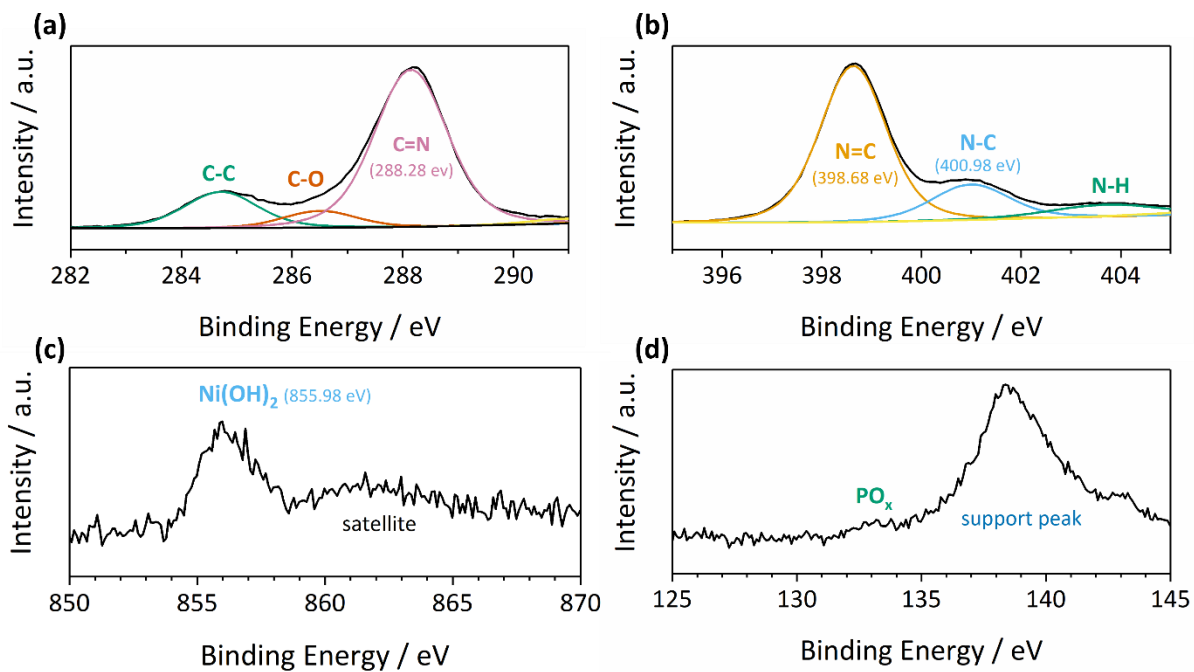
Figure S15. XPS spectra of the **(a)** C_{1s}, **(b)** N_{1s}, **(c)** Ni_{2p}, and **(d)** P_{2p} edges of used $CN_x|Ni_2P$ (2 wt%) after photoreforming. Photoreforming conditions: $CN_x|Ni_2P$ (3.2 mg), PLA (50 mg), 1 M aqueous KOH (2 mL), simulated solar irradiation (AM 1.5G, 100 mW cm^{-2}, 25 °C, 50 h).
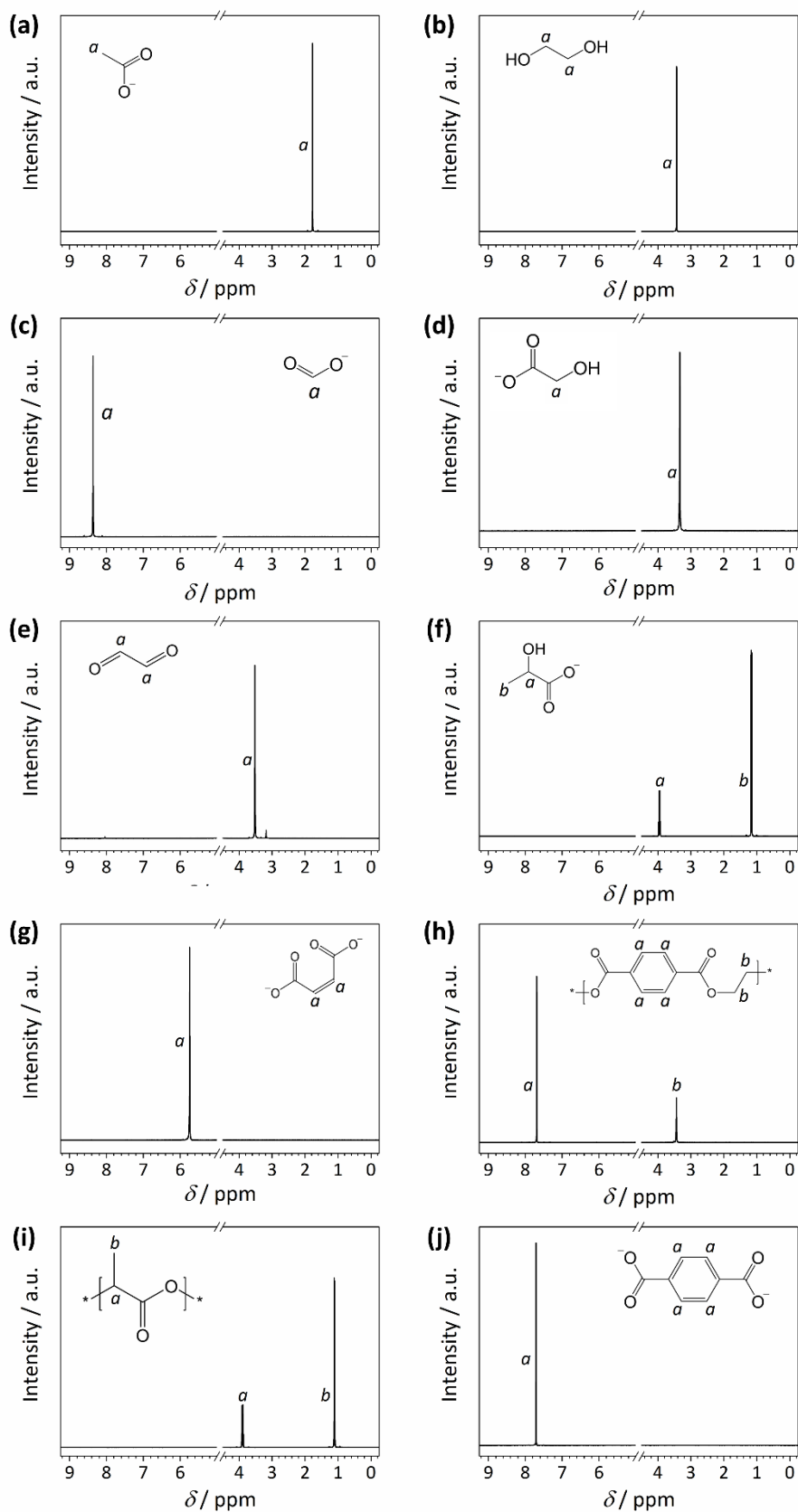
Figure S16. ^{1}H-NMR spectra of **(a)** acetate, **(b)** ethylene glycol, **(c)** formate, **(d)** glycolate, **(e)** glyoxal, **(f)** lactate, **(g)** maleate (used as a standard), **(h)** PET, **(i)** PLA, and **(j)** terephthalate in 1 M NaOD in D$_2$O. PET and PLA were pre-treated in 1 M NaOD in D$_2$O for 24 h before data collection.
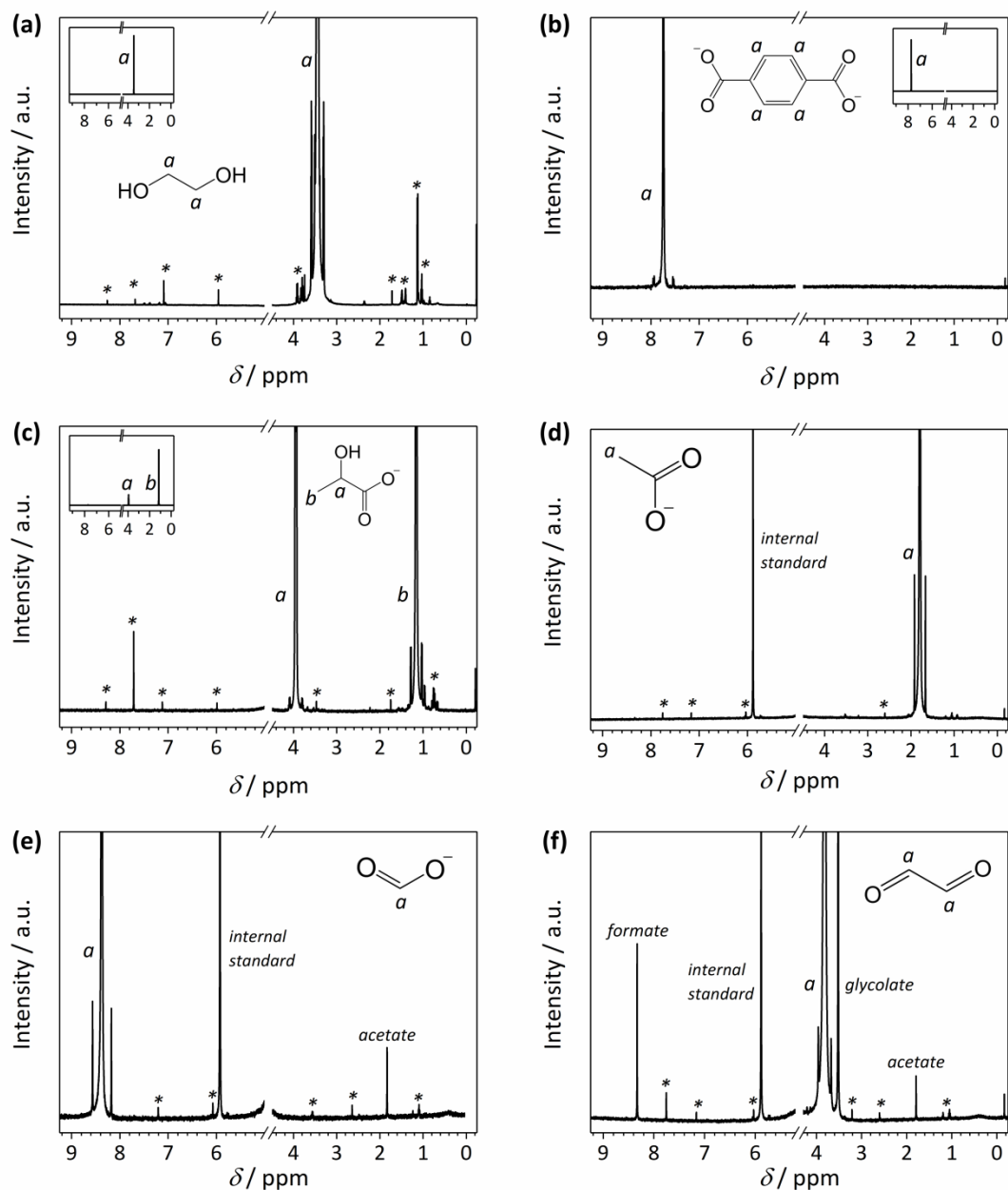
Figure S17. ^{1}H-NMR spectra of **(a)** ethylene glycol, **(b)** terephthalate, and **(c)** lactate after 5 days simulated solar light irradiation. ^{1}H-NMR spectra of **(d)** acetate, **(e)** formate and **(f)** glyoxal after 24 h simulated solar light irradiation. Maleic acid was used as an internal standard. Photoreforming conditions: $CN_x|Ni_2P$ 2 wt% (3.2 mg), NaOD (1 M) in D_2O (2 mL), substrate (25 mg mL^{-1}), irradiation (AM 1.5G, 100 mW cm^{-2}, 25 °C).
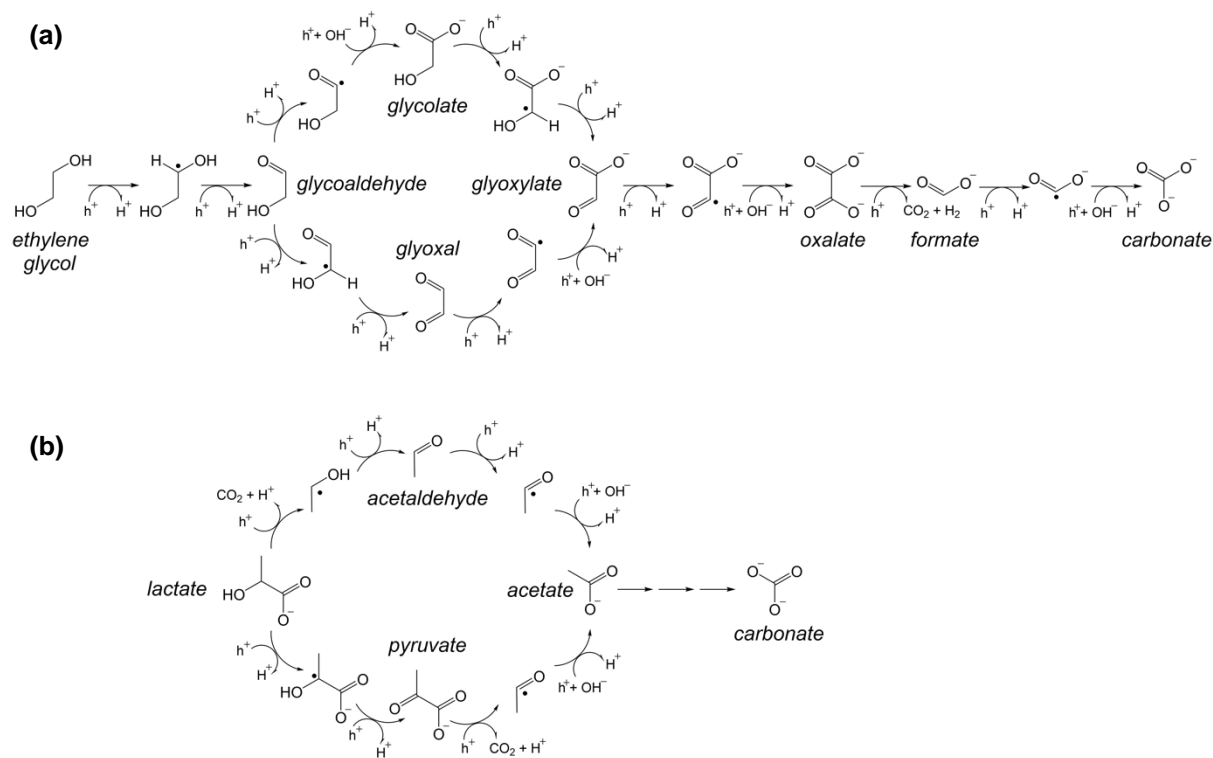
Figure S18. Proposed reaction scheme for the photo-oxidation of **(a)** ethylene glycol and **(b)** lactate. The mechanism is adapted from [14] and based on ^{1}H-NMR analysis and comparison to literature.[15–19]
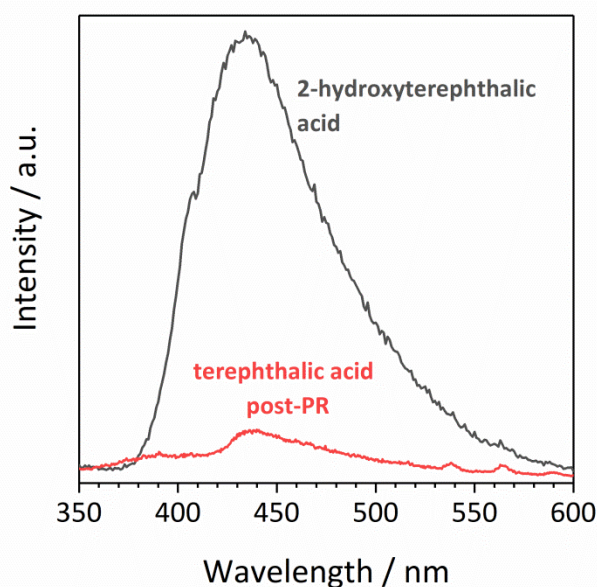
Figure S19. Emission spectra (λ_{ex} = 315 nm, λ_{em} = 430 nm) of pure 2-hydroxyterephthalic acid in 1 M aqueous KOH and terephthalic acid (50 mg) after photoreforming (AM 1.5G, 100 mW cm^{-2}, 25 °C, 20 h) with CN$_x$|Ni$_2$P (3.2 mg) in 1 M aqueous KOH (2 mL). Terephthalic acid does not exhibit the characteristic λ_{em} = 430 nm of the OH$^-$ scavenger 2-hydroxyterephthalic acid, indicating that OH$^-$ does not play a major role in the photoreforming mechanism.
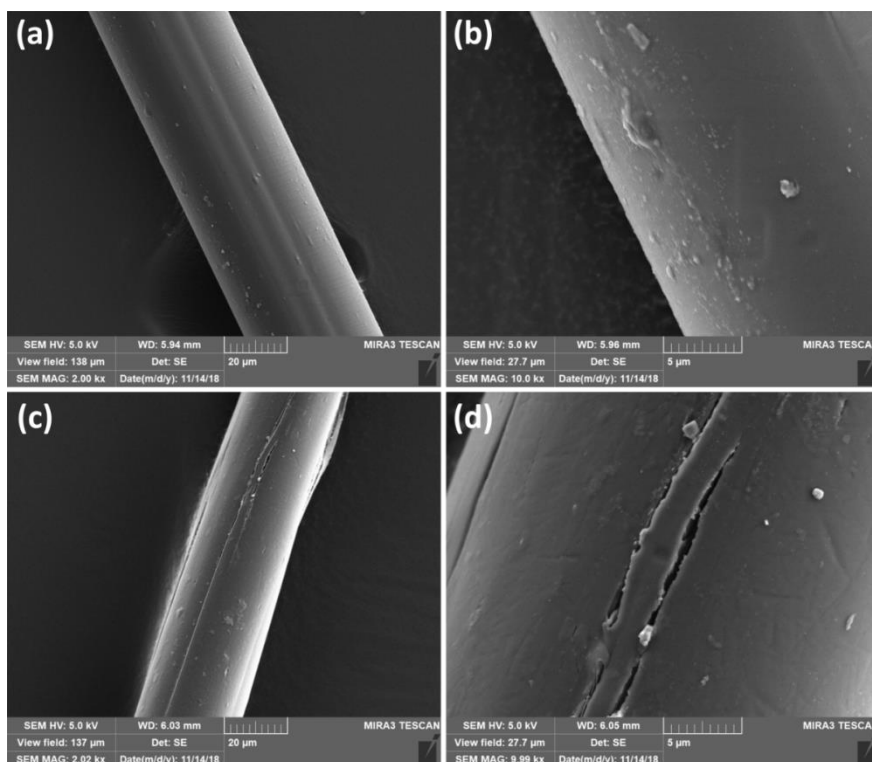
Figure S20. SEM images of a polyester microfiber **(a-b)** before photoreforming and **(c-d)** after photoreforming. Photoreforming conditions: $CN_x|Ni_2P$ (3.2 mg), 1 M KOH (2 mL), microfibers (10 mg), simulated solar irradiation (AM 1.5G, 100 mW cm^{-2}, 25 °C, 24 h). Reformed microfibers were washed with H_2O and dried under a stream of N_2. Both samples were sputter-coated with Pt (10 nm) prior to imaging.
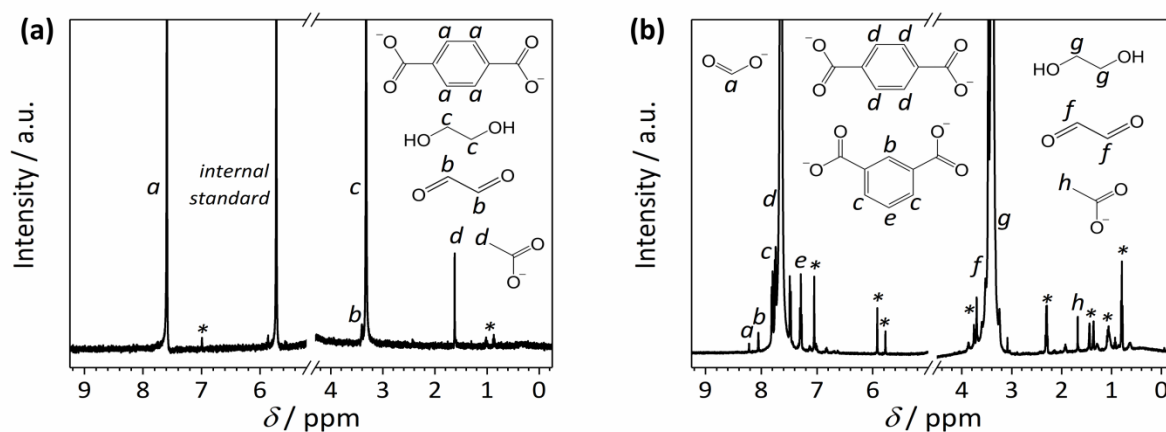
Figure S21. ^{1}H-NMR spectra of **(a)** polyester microfibers and **(b)** a PET water bottle after photoreforming. Photoreforming conditions: $CN_x|Ni_2P$ (3.2 mg), 1 M NaOD in D_2O (2 mL), pre-treated polymer (10 mg microfibers or 50 mg PET bottle), simulated solar irradiation (AM 1.5G, 100 mW cm^{-2}, 25 °C, 24 h).

References

(1)   Kawahara, Y.; Yoshioka, T.; Takarada, W.; Kikutani, T.; Tsuji, M. Alkaline Hydrolysis Kinetics of Poly (Ethylene Terephthalate) Fibers. *J. Fiber Sci. Technol.* **2016**, *72*, 9–16.

(2)   NIST Chemistry WebBook. 1,2-Ethanediol https://webbook.nist.gov/cgi/cbook.cgi?ID=C107211&Mask=2 (accessed Dec 4, 2018).

(3)   Diane Sylvie Chauliac. Development of a Thermochemical Process for Hydrolysis of Polylactic Acid Polymers to L-Lactic Acid and Its Purification Using an Engineered Microbe, University of Florida, 2013.

(4)   Emel'yanenko, V. N.; Verevkin, S. P.; Schick, C.; Stepurko, E. N.; Roganov, G. N.; Georgieva, M. K. The Thermodynamic Properties of S-Lactic Acid. *Russ. J. Phys. Chem. A* **2010**, *84*, 1491–1497.

(5)   Indra, A.; Acharjya, A.; Menezes, P. W.; Merschjann, C.; Hollmann, D.; Schwarze, M.; Aktas, M.; Friedrich, A.; Lochbrunner, S.; Thomas, A.; et al. Boosting Visible-Light-Driven Photocatalytic Hydrogen Evolution with an Integrated Nickel Phosphide-Carbon Nitride System. *Angew. Chem. Int. Ed.* **2017**, *56*, 1653–1657.

(6)   Lu, Z.; Li, C.; Han, J.; Wang, L.; Wang, S.; Ni, L.; Wang, Y. Construction 0D/2D Heterojunction by Highly Dispersed Ni_2P QDs Loaded on the Ultrathin $g-C_3N_4$ Surface towards Superhigh Photocatalytic and Photoelectric Performance. *Appl. Catal. B Environ.* **2018**, *237*, 919–926.

(7)   Ye, P.; Liu, X.; Iocozzia, J.; Yuan, Y.; Gu, L.; Xu, G.; Lin, Z. A Highly Stable Non-Noble Metal Ni_2P Co-Catalyst for Increased H_2 Generation by $g-C_3N_4$ under Visible Light Irradiation. *J. Mater. Chem. A* **2017**, *5*, 8493–8498.

(8)   Zeng, D.; Xu, W.; Ong, W.-J.; Xu, J.; Ren, H.; Chen, Y.; Zheng, H.; Peng, D.-L. Toward Noble-Metal-Free Visible-Light-Driven Photocatalytic Hydrogen Evolution: Monodisperse Sub–15 Nm Ni_2P Nanoparticles Anchored on Porous $g-C_3N_4$ Nanosheets to Engineer 0D-2D Heterojunction Interfaces. *Appl. Catal. B Environ.* **2018**, *221*, 47–55.

(9)   Zhao, H.; Sun, S.; Jiang, P.; Xu, Z. J. Graphitic C_3N_4 Modified by Ni_2P Cocatalyst: An Efficient, Robust and Low Cost Photocatalyst for Visible-Light-Driven H_2 Evolution from Water. *Chem. Eng. J.* **2017**, *315*, 296–303.

(10)   Wen, J.; Xie, J.; Shen, R.; Li, X.; Luo, X.; Zhang, H.; Zhang, A.; Bi, G. Markedly Enhanced Visible-Light Photocatalytic H_2 Generation over $g-C_3N_4$ Nanosheets Decorated by Robust Nickel Phosphide ($Ni_{12}P_5$) Cocatalysts. *Dalt. Trans.* **2017**, *46*, 1794–1802.

(11)   Yu, J.; Wang, S.; Cheng, B.; Lin, Z.; Huang, F. Noble Metal-Free $Ni(OH)_2$–$g-C_3N_4$ Composite Photocatalyst with Enhanced Visible-Light Photocatalytic H_2-Production Activity. *Catal. Sci. Technol.* **2013**, *3*, 1782.

(12)   Kawai, T.; Sakata, T. Photocatalytic Hydrogen Production from Water by the Decomposition of Poly-Vinylchloride, Protein, Algae, Dead Insects, and Excrement. *Chem. Lett.* **1981**, 81–84.

(13)   Uekert, T.; Kuehnel, M. F.; Wakerley, D. W.; Reisner, E. Plastic Waste as a Feedstock for Solar-Driven H_2 Generation. *Energy Environ. Sci.* **2018**, *11*, 2853–2857.

(14)   Puga, A. V. Photocatalytic Production of Hydrogen from Biomass-Derived Feedstocks. *Coord. Chem. Rev.* **2016**, *315*, 1–66.

(15)   Yue, H.; Zhao, Y.; Ma, X.; Gong, J. Ethylene Glycol: Properties, Synthesis, and Applications. *Chem. Soc. Rev. Chem. Soc. Rev* **2012**, *41*, 4089–4380.

(16)   Rossiter, W. J.; Brown, P. W.; Godette, M. The Determination of Acidic Degradation Products in Aqueous Ethylene Glycol and Propylene Glycol Solutions Using Ion Chromatography. *Sol. Energy Mater.* **1983**, *9*, 267–279.

(17)   Chauhan, N. L.; Dameera, V.; Chowdhury, A.; Juvekar, V. A.; Sarkar, A. Electrochemical Oxidation of Ethylene Glycol in a Channel Flow Reactor. *Catal. Today* **2018**, *309*, 126–132.

(18)   Lomate, S.; Katryniok, B.; Dumeignil, F.; Paul, S. High Yield Lactic Acid Selective Oxidation into Acetic Acid over a Mo-V-Nb Mixed Oxide Catalyst. *Sustain. Chem. Process.* **2015**, *3*, 5.

(19)   Harada, H.; Sakata, T.; Ueda, T. Effect of Semiconductor on Photocatalytic Decomposition of Lactic Acid. *J. Am. Chem. Soc.* **1985**, *107*, 1773–1774.

End of Supporting Information